Modeling Reliablity Issues in RF MEMS Switches

Gabriele Schrag, Thomas Künzig, Gerhard Wachutka
Institute for Physics of Electrotechnology
Munich University of Technology
Munich, Germany
schrag, kuenzig, wachutka@tep.ei.tum.de

***Abstract*— We present a problem-adapted, physics-based 3D finite element (FE) model of an RF-MEMS switch, which is used for investigating the failure scenario of such devices caused by electrically induced stiction, one of the major reliability concerns, which limits their broad commercial application as, e.g., in mobile phones. In particular, a novel embedded active thermal recovery capability is analyzed by coupled electro-thermo-mechanical simulations in order to identify those parameters, which are most significant for the recovery efficiency and, hence, provide the best prospects for optimizing the switch with a view to a reliable design. The derived model was validated and calibrated by optical white-light interferometry and laser Doppler vibrometry to make it reliable and accurate, particularly with regard to predictive simulation.**

Keywords—RF MEMS switch, problem-adapted modeling, 3D FE analysis, reliability, sticking

I. Motivation and Problem Description

For more than one decade, MEMS (Micro-Electro-Mechanical Systems) technology for Radio Frequency applications (RF-MEMS) has been proving its enormous potential for the fabrication of high performance and widely reconfigurable RF passive components such as tuneable filters [1], reconfigurable impedance matching networks [2], phase shifters [3], and high order switching matrices [4], applicable in modern commercial RF systems (e.g., mobile phones) for wireless telecommunication.

However, reliability of such devices is still a major concern on their way to market-readiness. An example is the design of RF-MEMS switches; here, the most scaring danger is sticking of the movable structural elements, which may lead to malfunctions or failure situations. Regarding electrostatically actuated devices (like the one depicted in Fig. 1), the two primary effects causing stiction are micro-welding (due to high local current densities within the RF signal [5]), and dielectric charging, i.e. accumulated charges, entrapped within the dielectric layers [6], which prevent the release of the switch.

In this work, an active recovery mechanism was investigated, which has been introduced and reported by [7]. It is supposed to be enabled in the case of the above described failure modes in order to restore the functionality of the switch. The entire switch design including the restoring facility and its operation is described in section II. The applied modeling methodology and the results obtained therefrom are presented in sections III and IV, respectively. The conclusions, which can be drawn from our investigations, are summarized in section V.

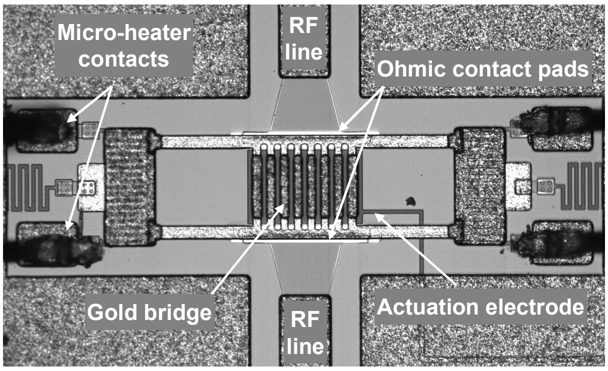

Fig. 1. Microphotograph of the RF MEMS switch under investigation. Meander-shaped resistive heaters are embedded underneath the anchors in order to recover the switch from potential failure modes.

II. Device Description and Working Principle

The RF MEMS switch under consideration has been fabricated by [7] and is depicted in the microphotograph of Fig. 1. The switch is composed of a movable slotted gold membrane suspended by four beams at the two anchor regions. It can be actuated applying a DC voltage between the membrane and the bottom electrode, which is buried between two oxide layers and connected to a DC Bias line. The electrostatic force pulls the gold membrane down towards the contact pads, thus closing the RF signal line. The above mentioned thermal recovery mechanism is realized by embedding meander-shaped polysilicon micro-heaters below each anchor (see Fig. 2).

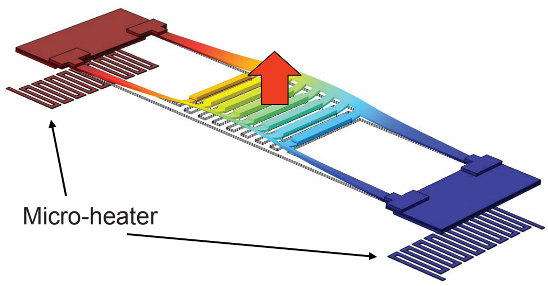

Fig. 2. Schematic view of the embedded recovery capability. Resistive micro-heaters underneath each anchor enable heating up the bridge in order to recover it from the failure mode.

During failure mode, a bias voltage is applied to one of the polysilicon meanders, causing an electric current, heating up parts of the device structure, and, thus, deforming the gold membrane through thermal expansion. As a consequence, the resulting bending forces are supposed to break up the welded contacts responsible for sticking. A further benefit of this design is that heating up the structures might also accelerate the discharging process within the dielectric layers, thus mitigating the second major effect causing stiction in electrostatic actuators.

The intention of the following investigations is to gain detailed insights in the behavior of the switch during failure, to study the basic functionality of the suggested recovery mechanism, to identify the most important parameters having impact on its efficiency and, finally, to derive guidelines for an improved and, hence, more robust design.

To this end, a model is required that is detailed enough to deliver insight into the device operation (internal heat propagation, e.g.) but, on the other hand, fast enough to allow for comprehensive design and optimization studies.

III. Model Derivation and Calibration

A physical model of the switch, which properly describes its operation and the recovery mechanism, and, thus, can be employed for virtually testing its efficiency and for deducing possible improvements of its design, has to include four different energy domains, namely mechanical, electrical, thermal, and viscous damping, as well as their mutual couplings.

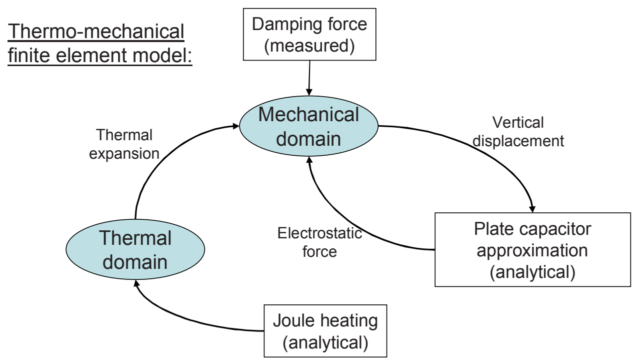

Fig. 3. Flow chart of the thermo-mechanical FE model. Electrical and fluidic effects are included as semi-analytical models.

In general, finite element analysis (FEA) is the method of choice for the detailed analysis of such MEMS devices. However, in the case of complex device geometries and several involved energy domains (as in the case of the switch considered) this method entails very long simulation times and weak convergence, and it may even become prohibitive, especially, when also transient effects have to be taken into account. Therefore, we derived a tailored, computationally efficient, but, at the same time, physics-based and predictive (i.e. scalable), coupled, semi-analytical 3D FE model following the coupling scheme depicted in Fig. 3. In order to make the problem tractable and to keep the computational expense in an affordable range, the Joule heating and the electrostatic actuation have been taken into account by introducing (semi-)analytical models, while the thermo-mechanical substructures are modeled by a coupled FEA. For further details of the model the reader is referred to [8].

All model parameters have been properly calibrated and validated by white-light interferometry and Laser Doppler vibrometry. The initial stress inside the movable membrane, for instance, has been extracted from the fundamental eigenfrequency at low ambient pressure and included in the mechanical model. Fluidic damping has been determined by measuring damped oscillations of the switch membrane under normal pressure conditions and, subsequently, included by introducing a constant damping factor. The gap underneath the gold membrane has been extracted from the optically measured quasi-static pull-in characteristics.

It turned out that special diligence has to be laid not only on the calibration of the absolute value of the process-induced stress inside the gold bridge, but also on its distribution along the layer thickness, which affects significantly the initial deformation. Fig. 4 shows the very good agreement between a 3D-profile of the MEMS switch as recorded by means of a white light interferometer and the simulated bending lines after performing a dedicated model calibration procedure.

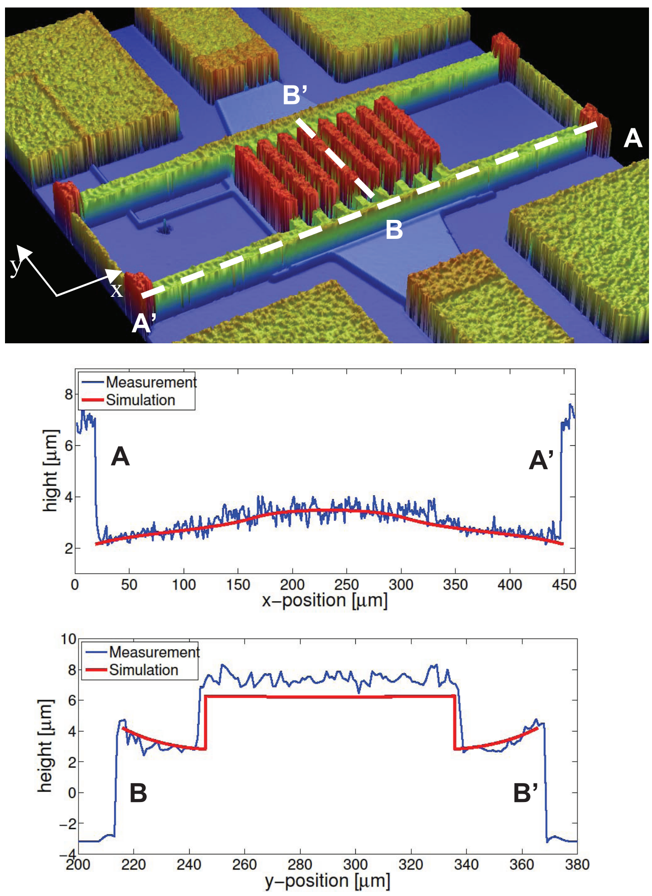

Fig. 4. 3D-profile of the MEMS switch as recorded by means of a white light interferometer. The deformation in the rest position is used to calibrate the initial stress distribution inside the gold bridge.

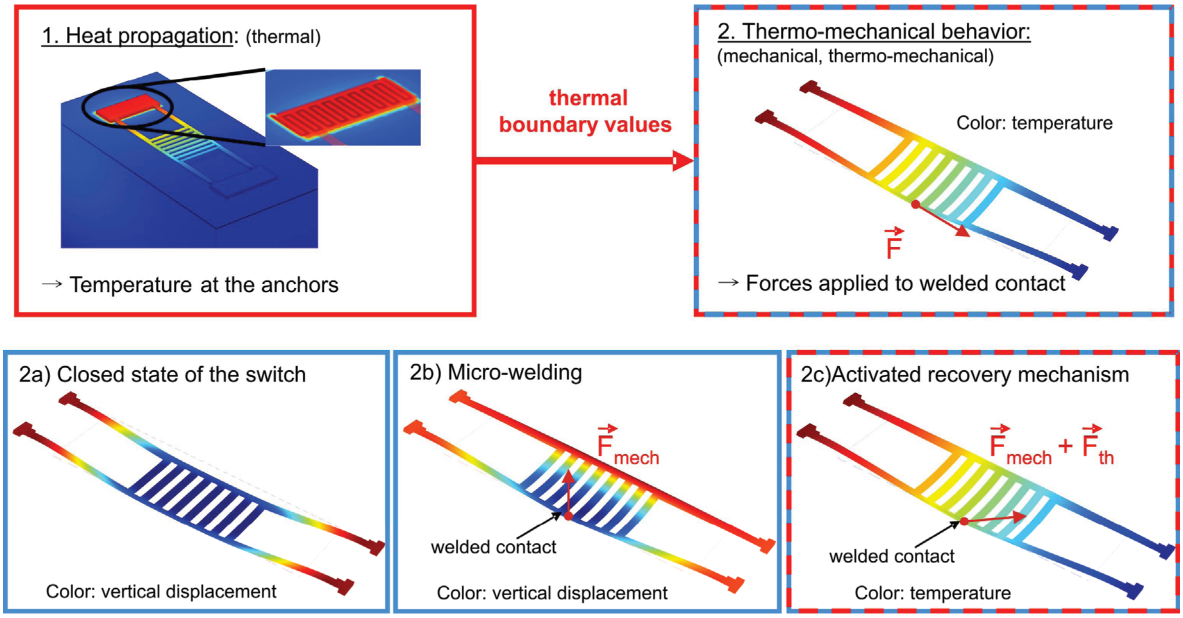

Fig. 5. Overview of the sequential simulation procedure applied to extract the thermally induced forces on potential welded contacts. The colors of the boxes refer to the respective type of simulation (red: thermal, blue: mechanical, red-blue: thermo-mechanical).

The calibrated and validated model can now be used to evaluate the restoring mechanism in the failure scenario, viz. the temperature distribution and the thermally induced forces exerted on potential welding spots. To this end, the sequential simulation procedure depicted in Fig. 5 has been developed. A pure thermal FE analysis of the device including also the substrate (step 1) delivers the temporal evolution of the temperature distribution. Step 2 comprises first a pure mechanical contact simulation (2a) to calculate the deformation of the switch in its closed position by applying an electrostatic force. Then the restoring mechanical force on a fixed contact point is extracted (2b). Finally, the transient temperature distribution extracted from step 1 enters the thermo-mechanical model (step 2c) as boundary condition and the total force acting on the welded contact is extracted. Subtracting the mechanical restoring force (calculated by step (2b)) from the so-determined value of the total force, we obtain the force exerted solely by the thermal recovery facility, and, thus, an estimate of its effectiveness during a potential failure situation.

IV. Model Validation and Simulation Results

Since the heat propagation inside the device is a crucial point for the effectiveness of the recovery facility, which cannot be assessed directly through measurements, the above-described thermo-electro-mechanical modeling approach has been verified by comparing the simulated thermally induced steady-state and transient deflections of the bridge with optically measured data (Figs. 6 and 7). The very good accordance between simulated and measured values illustrates the high reliability level of the derived model for the subsequent investigations, where important factors impacting the functionality of the recovery facility are identified in order to estimate the potential for optimization of the design with a view to improving the robustness against sticking-induced failure.

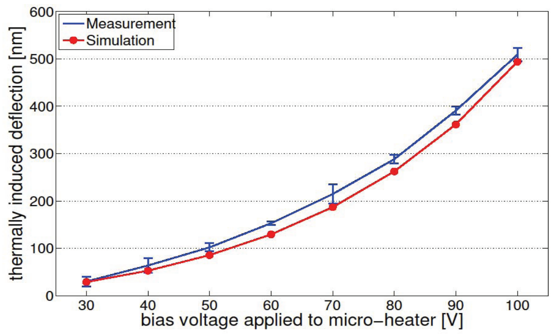

Fig. 6. Thermally induced vertical deflection of the bridge for different bias voltages applied to the heater.

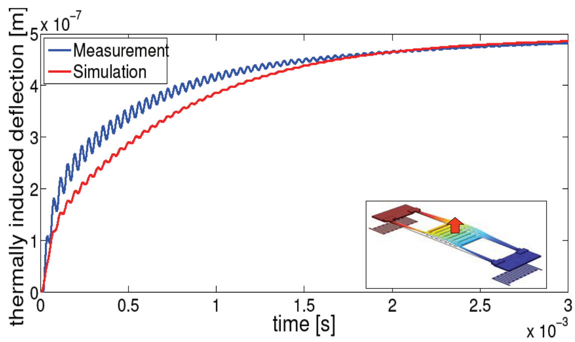

Fig. 7. Transient thermal expansion of the gold bridge. Both simulation and measurement show a superimposed oscillation at the mechanical resonance frequency of the bridge.

The so-derived and validated physics-based model combines short simulation times with detailed insights in the switch operation such as the temperature evolution inside the device (Fig. 8). It can be seen that the major temperature rise occurs inside the switch membrane and the hot anchor, but, on the other hand, the largest portion of the entire heat is propagating into the substrate. This emphasizes the decisive role of the oxide layers between anchor and substrate as design parameter to tune the heating efficiency. As a consequence of this finding, the thermally induced forces increase proportionally with increasing the thickness of the oxide layer underneath the heater (field oxide).

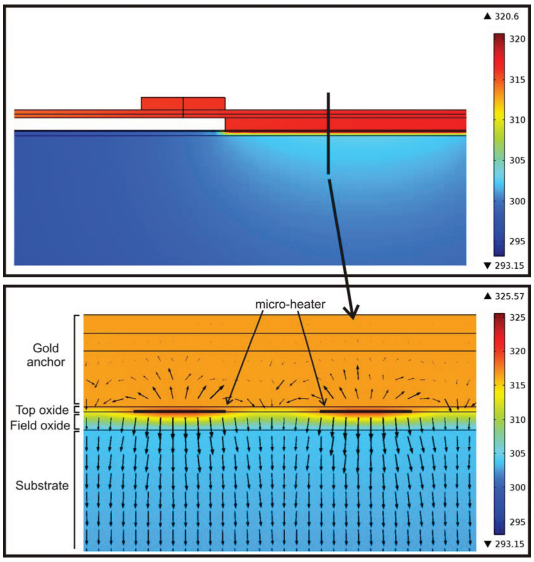

Fig. 8. Stationary temperature distribution on two cross-sections through the switch at the hot anchor as obtained by 3D FEA. The black arrows indicate the heat flux.

Another result obtained by this model is the total force and, therefrom, the amount of the thermally induced force exerted by the activated heaters on a potential adhesion point depending on the lateral position on the bridge, which is depicted in Fig. 9 (for a slightly modified switch design). As expected, the mechanical restoring force shows no dependence on the position, while the thermally induced force is varying slightly along the bridge due to the fact that its value is correlated with the relative volume dilatation.

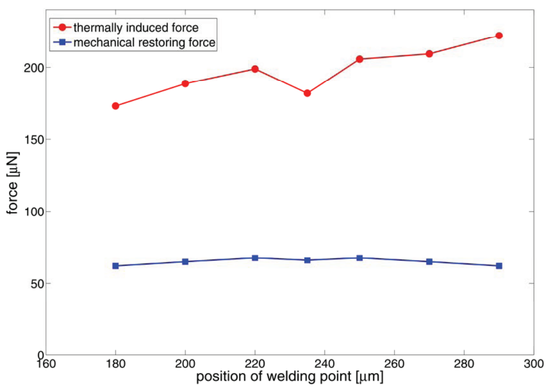

Fig. 9. Mechanical and thermally induced forces acting on a welded contact as a function of the distance from the hot anchor.

However, the maximum variation is only of about 25%, and, hence, shows no dramatic dependence. Additionally, the total value of the forces exerted on potential sticking points can be evaluated to lie between about 180 µN to 220 µN. This value constitutes a promising result, since it is of the same order as those reported for welded gold contacts (100 µN -400 µN) [7], which, in principle, proves the basic functionality of the considered design.

V. Conclusions

We demonstrated a problem-adapted, efficient FE-based modeling procedure including the cross-coupling between all relevant energy domains, which allows for the detailed investigation of RF MEMS switches in the case of failure situations caused by stiction. Applying this model, we demonstrated the basic functionality of a novel thermal recovery facility and identified the parameters, which have a decisive impact on the efficiency of the recovery and, hence, offer the potential for further improvements towards a more robust switch design. The very good agreement between the measured and the simulated static and transient characteristics demonstrates the high confidence level of the model and its potential for predictive simulation as a part of a design optimization loop with a view to improving the robustness of the device against failure.

References

[1] A. Malczewski, B. Pillans, F. Morris, R. Newstrom, "A family of MEMS tunable filters for advanced RF applications", Proc. of International Microwave Symposium 2011, pp.1-4.

[2] F. Domingue, S. Fouladi, R. Mansour, "A reconfigurable impedance matching network using dual-beam MEMS switches for an extended operating frequency range", Proc. of International Microwave Symposium 2010, pp 1552-1555.

[3] B. Belenger, B. Espana, S. Courreges, P. Blondy, O. Vendier, D. Langrez, J.-L. Cazaux, "A high-power Ka-band RF-MEMS 2-bit phase shifter on Sapphire substrate", Proc. of Microwave Integrated Circuits Conf. 2011, pp 164-167.

[4] M. Daneshmand, R. Mansour, « RF MEMS Satellite Switch Matrices", IEEE Microwave Magazine. 12-5, 2011, pp. 92-109.

[5] A. Tazzoli, J. Iannacci, G. Meneghesso, "A positive exploitation of ESD events: Micro-welding induction on ohmic MEMS contacts", Proc. of the Electrical Overstress/Electrostatic Discharge Symp. 2011, pp 1-8.

[6] W. M. van Spengen, R. Puers, R. Mertens, I. De Wolf, "A comprehensive model to predict the charging and reliability of capacitive RF MEMS switches", J. Micromech. Microeng., Vol. 14 2004, pp. 514-521

[7] J. Iannacci, A. Faes, A. Repchankova, A. Tazzoli, G. Meneghesso, "An active heat-based restoring mechanism for improving the reliability of RF-MEMS switches", Journal of Microelectronics Reliability. 51-9/11, 2011, pp. 1869-1873

[8] T. Kuenzig, J. Iannacci, G. Schrag, G. Wachutka, "Study of an active thermal recovery mechanism for an electrostatically actuated RF-MEMS switch", Proc. of 13th Intern. Conference on Thermal, Mechanical and Multi-Physics Simulation and Experiments in Microelectronics and Micro-Systems (EuroSime), 2012.